J. Am. Chem. Soc. **1993,** *115,* 4201–4209 4201

# Valence Bond Concepts Applied to the Molecular Mechanics Description of Molecular Shapes. 1. Application to Nonhypervalent Molecules of the P-Block

**Daniel M. Root, Clark R. Landis,* and Thomas Cleveland**

*Contribution from the Department of Chemistry, University of Wisconsin, Madison, Wisconsin 53706*

*Received October 30, 1992*

**Abstract:** Most molecular mechanics methods attempt to describe accurate potential energy surfaces by using a variant of the general valence force field (commonly using the diagonal terms, only) and a large number of parameters. However, these simple force fields are not accurate outside the proximity of the energetic minima and often are difficult to apply to the different shapes and higher coordination numbers of, for example, transition metal complexes. As the application of molecular mechanics methods is extended to collections of atoms that span the entire periodic table, the requisite number of parameters rapidly becomes unmanageable. For this work, we adopt readily derived hybrid orbital strength functions as the basis for a molecular mechanics expression of molecular shapes. These functions are suitable for accurately describing the energetics of distorting bond angles not only around the energy minimum but also for very large distortions as well. The combination of these functions with simple valence bond ideas (such as Bent's rule) leads to a simple scheme for predicting molecular shapes. Structures and vibrational frequencies calculated by the VALBOND program agree well with experimental data for a variety of molecules from the main group of the periodic table. Overall the qualities of the results are similar to those of other popular force fields (such as MM3) despite the use of fewer angular parameters.

## I. Introduction

Molecular mechanics methods are accurate and rapid tools for the evaluation of molecular structures, energetics, and dynamics.[1] Although the bulk of molecular mechanics applications has concerned carbon-based molecular structures such as proteins, there has been a steadily growing interest in applying molecular mechanics computations to a broader range of compounds, e.g., transition metal complexes.[2] However, both the form of the potential energy expression in molecular mechanics and the daunting prospect of developing parameters for atom combinations from throughout the periodic table limits the extension of molecular mechanics.[3]

All molecular mechanics computational activities evolve from the formulation of the potential energy expression or force field. Beginning with the foundation-laying work of Westheimer[4] and continuing through today, the functional form of the potential energy expressions used by molecular mechanics packages are extensions of the valence force field first introduced by Bjerrum.[5] Simple valence force fields, as employed in popular molecular mechanics programs, express the molecular potential energy as a sum of bonded terms—bond stretching, angle bending, proper torsions, and improper torsions—and nonbonded terms—van der Waals and electrostatic interactions—for atom pairs that are not connected by one or two bonds. As an example, the potential energy expression utilized by the CHARMM program[6] is given in 1. Other popular molecular mechanics programs are similar

$$E = \sum^{\text{bonds}} k_r(r-r_0)^2 + \sum^{\substack{\text{bond}\\ \text{angles}}} k_\theta(\theta-\theta_0)^2 + \sum^{\substack{\text{improper}\\ \text{torsions}}} k_\varphi(\varphi-\varphi_0)^2 + \sum^{\substack{\text{proper}\\ \text{torsions}}} k_\psi(1+\cos(n\psi+\delta)) + \text{electrostatic terms} + \text{van der Waals terms} \quad (1)$$

to the CHARMM force field. It should be noted that the force fields commonly used for detailed vibrational analysis contain more terms in the force field in order to fit more precisely the experimental data. The MM3 force field[7] is a compromise between the full vibrational force fields and the simple diagonal force field of eq 1. Impressively, MM3 simultaneously reproduces molecular structures, vibrational frequencies, and conformational energetics albeit at the expense of a large parameter set.

Previously, we have described some of the difficulties that arise when these simple valence force fields are applied to the more complex shapes of transition metal complexes.[8] In summary, these difficulties include (1) the inadequacy of harmonic functions for describing the energetics of bond angle distortions far from the energy minimum, particularly in the bond angle region near 180° and (2) the multiplicity of equilibrium bond angles that may occur in, for example, square planar complexes for which both 90° and 180° equilibrium bond angles are required for the same atom combinations. In order to avoid some of these problems, we developed the SHAPES force field which is based on angular overlap considerations.

Recently, great strides have been made by Rappé, Casewit, and co-workers[3] on the problem of parametrizing molecular mechanics force fields. The UFF molecular mechanics force field as well its precursor, the Dreiding force field, simplifies parametrization through the use of general rules and atom-based parameters. For example, bond stretch and angle bend force constants are derived from generalizations of Badger's rules. Bond length parameters are derived from covalent radii that are

---

[1] Allinger, N. L.; Burkert, U. *Molecular Mechanics*; American Chemical Society: Washington, DC 1982.

[2] (a) Castonguay, L. A.; Rappé, A. K.; Casewit, C. J. *J. Am. Chem. Soc.* **1991**, *113*, 7177. (b) Timofeeva, T. V.; Struchkov, Y. T. *Russ. Chem. Rev.* **1990**, *59*, 320. (c) Castonguay, L. A.; Rappé, A. K. *J. Am. Chem. Soc.* **1992**, *114*, 5832. (d) Lin, Z.; Marks, T. J. *J. Am. Chem. Soc.* **1990**, *112*, 5515. (e) Hay, B. P. *Inorg. Chem.* **1991**, *30*, 2876. (f) Brubaker, G. R.; Johnson, D. W. *Coord. Chem. Rev.* **1984**, *53*, 1. (g) Sironi, A. *Inorg. Chem.* **1992**, *31*, 2467. (h) Doman, T. N.; Landis, C. R.; Bosnich, B. *J. Am. Chem. Soc.* **1992**, *114*, 7264.

[3] Rappé, A. K.; Casewit, C. J.; Colwell, K. S.; Goddard III, W. A.; Skiff, W. M. *J. Am. Chem. Soc.* **1992**, *114*, 10024.

[4] Westheimer, F. H.; Mayer, J. E. *J. Chem. Phys.* **1947**, *15*, 252.

[5] Bjerrum, N. *Verhandl. Deut. Physik. Ges.* **1914**, *16*, 737.

[6] Brooks, R.; Bruccoleri, R. E.; Olafson, B. D.; States, D. J.; Swaminathan, S.; Karplus, M. *J. Comput. Chem.* **1983**, *4*, 187.

[7] Allinger, N. L.; Yuh, Y. H.; Lii, J.-H. *J. Am. Chem. Soc.* **1989**, *111*, 8551.

0002-7863/93/1515-4201$04.00/0

corrected for bond orders and electronegativity effects. In the UFF force field, equilibrium bond angles are set by the coordination number, e.g., an oxygen with two ligands attached is assumed to have an equilibrium bond angle of 104.5°. Other workers have simplified the parametrization of molecular mechanics angle bending terms by removing the bending term altogether and replacing them with ligand–ligand van der Waals terms.[2b,9]

This paper focuses on the derivation of a new molecular mechanics force field formulation of angle bending terms that is based on the principles of simple valence bond theory. As in our previous work we focus on bending terms because they determine the molecular shape and, hence, address a crucial need in the extension of molecular mechanics to many inorganic complexes. In the following sections we present (1) the derivation of hybrid orbital strength functions, (2) the formulation of force field terms incorporating hybrid orbital strength functions, (3) a connectivity based algorithm for assigning hybridizations, and (4) a comparison of experimental geometries and vibrational frequencies with those computed by the force field. Simple molecules conforming to nonhypervalent Lewis structures are treated in this work; hypervalent molecules and transition metal complexes will be the subject of subsequent publications.

## II. Generalized Hybrid Orbital Strength Functions

Pauling's landmark 1931 paper[10] established the fundamental principles of the directed covalent bond: (1) the bond is formed through the interaction of two unpaired electrons on each of the atoms and (2) for a given eigenfunction, the bond will tend to be formed in the direction with the largest value of the eigenfunction. By proposing changes in the quantization of atomic eigenfunctions, i.e., hybridization, as a mechanism for forming the strongest possible bonds, Pauling derived the set of equivalent and orthogonal hybrids that permit the formation of four equivalent bonds in methane. These $sp^3$ hybrid orbitals point to the corners of a regular tetrahedron, thus providing theoretical justification of the tetrahedral geometry of methane. Similarly, $sp^2$ hybrids have maxima pointing to the corners of an equilateral triangle, and sp hybrids have maxima pointing in opposite directions along a line. Indeed, the correlation of hybridization with geometry ($sp^3 \approx$ tetrahedral, $sp^2 \approx$ trigonal planar, sp $\approx$ linear) is so powerful and so ingrained in our chemical training that we frequently use hybridization to describe geometry and vice versa.

Molecular mechanics computation begin with the specification of a bonded topology, i.e., the user must specify which atoms are connected by localized bonds. This topology then determines whether specific atom–atom interactions are to be treated with bonded or nonbonded terms. Thus, molecular mechanics computations conceptually are associated more readily with the localized bonds formed by overlap of hybrid orbitals than with the delocalized bonds formed by linear combinations of atomic orbitals according to molecular orbital theory. By this reasoning, the angular dependence of the bond-forming power, or strength, of hybrid orbitals is an attractive starting point for the derivation of angle bending terms in molecular mechanics.

Our derivation of a general expression for the strength of hybrid orbitals follows that of Pauling[11] and is illustrated first for $sp^3$ hybrid orbitals. Let $hy_1$ and $hy_2$ represent equivalent $sp^3$ hybrid orbitals with the maximum value of $hy_1$ lying along the $z$-axis (eq 2). The strength, $S$, of this orbital is given by the value of the angular part of the eigenfunction at its maximum. For an $sp^3$ orbital, $S = 2$. A second $sp^3$ hybrid orbital, $hy_2$ (eq 3), may be constructed in the $xz$ plane that makes an angle $\alpha$ with $hy_1$. These orbitals are not necessarily orthogonal and the nonorthogonality, or overlap, integral ($\Delta$) may be computed readily (eq 4).

$$hy_1 = \frac{1}{2}(1s + \sqrt{3}p_z) \tag{2}$$

$$hy_2 = \frac{1}{2}(1s + \sqrt{3}(\cos \alpha p_z + \sin \alpha\, p_x)) \tag{3}$$

If the orbitals are not orthogonal their strengths will decrease from the

$$\Delta = \frac{1}{4}(1 + \sqrt{3}\cos \alpha) \tag{4}$$

maximum value of 2. Pauling showed that the decrease in the hybrid orbital strengths can be related to the nonorthogonality integrals. By assuming that the nonorthogonal hybrid orbitals can be expressed as linear combinations of equivalent, orthogonal orbitals, $\psi_1$ and $\psi_2$ (eqs 5 and 6), the coefficients of these orthogonal

$$hy_1 = \beta\psi_1 + \sqrt{(1-\beta^2)}\psi_2 \tag{5}$$

$$hy_2 = \sqrt{(1-\beta^2)}\psi_1 - \beta\psi_2 \tag{6}$$

hybrid orbitals can be expressed in terms of $\Delta$ (eqs 7 and 8). For

$$\psi_1 = \frac{\beta hy_1 - \sqrt{(1-\beta^2)}hy_2}{2\beta^2 - 1} \tag{7}$$

$$\beta^2 = \frac{1 - \sqrt{(1-\Delta^2)}}{2} \tag{8}$$

$sp^3$ hybrids having bond angle $\alpha$ the strength of the orbitals, $S(\alpha)$, in the direction of their maxima is related to the

$$S(\alpha) = S^{max}\sqrt{1 - \frac{1 - \sqrt{1-\Delta^2}}{2}} \tag{9}$$

nonorthogonality integral as shown below, where $S^{max}$ is the maximum possible strength of the orbits. For $sp^3$ hybrids the value of $S^{max}$ is 2. The interpretation of the quantity

$$\sqrt{1 - \frac{1 - \sqrt{1-\Delta^2}}{2}}$$

is that it represents the fractional decrease in strength of the two $sp^2$ hybrids placed at angle $\alpha$ due to their nonorthogonality at that angle. Placing two $sp^3$ orbitals at any angle other than the tetrahedral angle (109.4°) decreases the value of their angular parts along the bond directions because the hybrid orbitals must be orthogonal. At the tetrahedral angle these hybrid orbitals have maximum strength, but at larger angles the strength decreases and reaches a plateau at 180°. At smaller angles the strength decreases rapidly as shown in Figure 1.

We have found that for equivalent hybrid orbitals of the form $sp^md^n$ making the angle $\alpha$ with one another, the orbitals and the angular dependence of their strength functions are given by the following expressions (eqs 10–13) and by eq 9. For example, the strength functions for $sp^2$, sp, and pure p orbitals are shown in Figure 1. These strength functions have maxima at 120°, 180°, and 90° with values of 1.991, 1.932, and 1.732, identical to those derived from other methods. Similarly, the generalized strength function of (eq 13) is identical to Pauling's $sp^3d^5$ function when $m = 3$ and $n = 5$. Therefore, we conclude that this generalized hybrid orbital strength is useful for expressing the angular dependence of all hybrid orbital types.

Strength refers to the value of the angular part of the function and represents a concentration of electron density in the bond-forming region. Therefore, the strengths of hybrid orbitals have

---

(8) Allured, V. S.; Kelly, C. M.; Landis, C. R. *J. Am. Chem. Soc.* **1991**, *113*, 1.

(9) Gajewski, J. J.; Gilbert, K. E.; McKelvey, J. *Advances in Molecular Modelling*; Liotta, D., Ed.; JAI Press: Greenwich, CT 1990, Vol. 2, p 65.

(10) Pauling, L. *J. Am. Chem. Soc.* **1931**, *58*, 1367.

(11) Pauling, L. *Proc. Natl. Acad. Sci. U.S.A.* **1976**, *73*, 274.

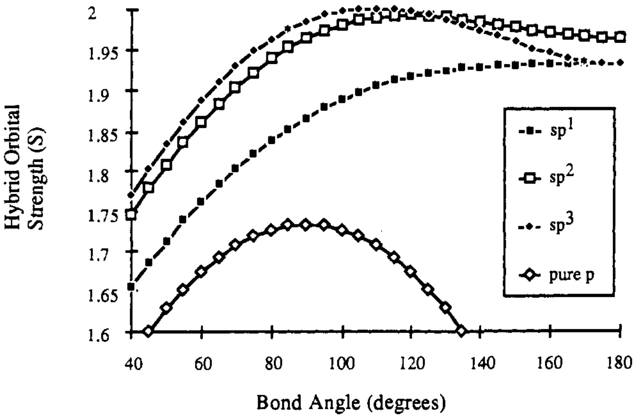

**Figure 1.** Strength functions for sp$^3$, sp$^2$, sp$^1$, and pure p orbitals.

$$\mathrm{hy}_1 = \sqrt{\frac{1}{1+m+n}}(1\mathrm{s} + \sqrt{m}p_z + \sqrt{n}\mathrm{d}z^2) \quad (10)$$

$$\mathrm{hy}_2 = \sqrt{\frac{1}{1+m+n}}\Big(1\mathrm{s} + \sqrt{m}(\cos\alpha \mathrm{p}_z + \sin\alpha \mathrm{p}_x) + \sqrt{n}\Big(\frac{1}{2}(3\cos^2\alpha - 1)\mathrm{d}z^2 + \frac{\sqrt{3}}{2}\sin^2\alpha \mathrm{d}x^2 - y^2 + \sqrt{3}\sin\alpha\cos\alpha \mathrm{d}xz\Big)\Big) \quad (11)$$

$$\Delta = \frac{1}{1+m+n}\Big(1s + m\cos\alpha p_z + \frac{n}{2}(3\cos^2\alpha - 1)\mathrm{d}z^2\Big) \quad (12)$$

$$S^{\max} = \sqrt{\frac{1}{1+m+n}}(1 + \sqrt{3m} + \sqrt{5n}) \quad (13)$$

been interpreted as synonymous with the bond-forming power of the orbitals. It is tempting to correlate hybrid orbital strengths with the bond dissociation energies.[12] The correlation is poor, however, as the values presented above would suggest that bonds involving sp$^3$ hybrids are stronger than those employing sp$^2$ or sp hybrid orbitals.[13] Experimental measurements of C–H bond strengths for alkanes, alkenes, and alkynes exhibit the opposite trend. One shortcoming of the hybridization procedure presented above is that the radial components of the orbitals have been ignored. The sp hybrid orbitals may be considered to give stronger C–H bonds because the radial overlap is increased. The hybrid orbitals that we use are based on the angular part of the wave function, only. These geometry-based hybridizations are not equivalent to the "truer" hybridizations revealed by methods that consider both the radial and angular parts of the orbitals. Thus, one should not expect our hybridizations to be the same as hybridizations obtained from accurate valence bond computations[14] or from the localization of good molecular orbital wave functions.[15]

With these limitations acknowledged, we propose that geometry-based hybrid orbital strength functions are appropriate functions for the angular terms of force fields. Let us assume that the strength of a pair of equivalent bonding hybrid orbitals varies with bond angle according to 9. For water, with an equilibrium bond angle of 104.5°, the appropriate hybridization is sp$^{3.88}$. If we set the energy of the equilibrium geometry equal to zero, the potential energy expression is given by 14. At nonequilibrium geometries, each of the hybrid orbitals forming O–H bonds contains defects due to nonorthogonality. Multiplication of these defects by a scaling factor ($k$) and summation over the two hybrid orbitals generates the potential energy curve shown in Figure 2. Intuitively, this curve is seen to have the proper shape: it increases rapidly as the bond angle is made smaller and the ligand separation decreases. At larger bond angles the energy increases and then levels to zero slope at 180°. This function satisfies more than just intuition. Adjustment of the scaling factor ($k$) to give the correct bending vibrational frequency leads to a curve that is nearly identical to that computed at the Hartree–Fock level,[16] also shown in Figure 2. Potential energy curves for a variety of X–Y–X molecules where Y are group VI (or 16) atoms are presented in Figure 3. For each molecule the curves for the hybridization-based energies are well-behaved and nearly indistinguishable from those computed at the Hartree–Fock level.

$$E = k(S^{\max}_{\mathrm{hy}_1} - S_{\mathrm{hy}_1}(\alpha)) + k(S^{\max}_{\mathrm{hy}_2} - S_{\mathrm{hy}_2}(\alpha)) \quad (14)$$

Up to this point we have demonstrated that hybrid orbital strength functions have the proper shapes for describing simple bending potential energy surfaces for molecules having two identical ligands. The essential relationship is that the molecular energy is related to the defects in the hybrid orbital strengths relative to the maximum strength for the preferred hybridizations. For molecules with more than two inequivalent ligands, we must address (1) how the defects should be computed and (2) how the preferred hybridizations are determined.

## III. Summation of Hybrid Defects for Multiple Ligands

For complex molecules having more than two ligands, Pauling proposed a pair defect approximation (PDA) as a method for estimating the net strength of hybrid orbitals.[17] For more than two equivalent ligands the defect for a hybrid orbital, $S^{\max} - S(\alpha)$, where $S(\alpha)$ is computed according to 9, is summed over all ligand angles made with that orbital. We use a similar procedure for the angular potential energy expression. For example, in ammonia the energy due to loss of strength of the hybrid orbital pointing to the first hydrogen is given by 15. The total energy due to angular distortion is simply the sum of the energies for the three ligand hybrids (eq 16). Figure 4 illustrates the contour plots computed at the Hartree–Fock level and using the strength functions for angular distortions of ammonia. As with the X–Y–X molecules, the two potential energy surfaces are nearly identical.

$$E_{\mathrm{hy}_1} = k(S^{\max}_{\mathrm{hy}_1} - S_{\mathrm{hy}_1}(\alpha_{1,2})) + k(S^{\max}_{\mathrm{hy}_1} - S_{\mathrm{hy}_1}(\alpha_{1,3})) \quad (15)$$

$$E_{\mathrm{tot}} = E_{\mathrm{hy}_1} + E_{\mathrm{hy}_2} + E_{\mathrm{hy}_3} \quad (16)$$

If the ligands are not all identical, the different preferred hybridizations for the inequivalent ligands must be accommodated. Bent[18] previously has proposed that variations in bond angles and other molecular properties can be rationalized in terms of the preference of the ligand for hybrid orbital p-character. This proposal commonly is referred to as Bent's rule. For chloroform, the experimental Cl–C–Cl bond angles are ca. 110.4°, and the H–C–Cl bond angles are ca. 108.5°. These angles correspond to hybridizations of sp$^{2.8}$ for the C–Cl bond-forming hybrids and sp$^{3.75}$ for the C–H bond-forming hybrid orbital. With individual bond hybridizations identified, the computation of the total angular energy uses the sp$^{3.75}$ strength function for each of the C–H bonds and sp$^{2.8}$ for the C–Cl bonds (see Figure 5). Note that the computation of, for example, the approximated defect of the C–H hybrid orbital depends only on the hybridization of

---

(12) Pauling, L. *The Nature of the Chemical Bond*, 2nd ed.; Cornell University Press: Ithaca, NY, 1960.

(13) Coulson, C. A. *Valence*, 2nd ed.; Oxford University Press: London, 1961.

(14) Goddard III, W. A.; Harding, L. B. *Ann. Rev. Phys. Chem.* **1978**, *29*, 363.

(15) Foster, J. P.; Weinhold, F. *J. Am. Chem. Soc.* **1980**, *102*, 7211.

(16) Gaussian92, Revision A, Frisch, M. J.; Trucks, G. W.; Head-Gordon, M.; Gill, P. M. W.; Wong, M. W.; Foresman, J. B.; Johnson, B. G.; Schlegel, H. B.; Robb, M. A.; Replogle, E. S.; Gomperts, R.; Andres, J. L.; Raghavachari, K.; Binkley, J. S.; Gonzalez, C.; Martin, R. L.; Fox, D. J.; Defrees, D. J.; Baker, J.; Stewart, J. J. P.; Pople, J. A. Gaussian, Inc.: Pittsburgh, PA, 1992.

(17) Pauling, L. *Proc. Natl. Acad. Sci. U.S.A.* **1975**, *72*, 4200.

(18) Bent, H. *Chem. Rev.* **1961**, 275.

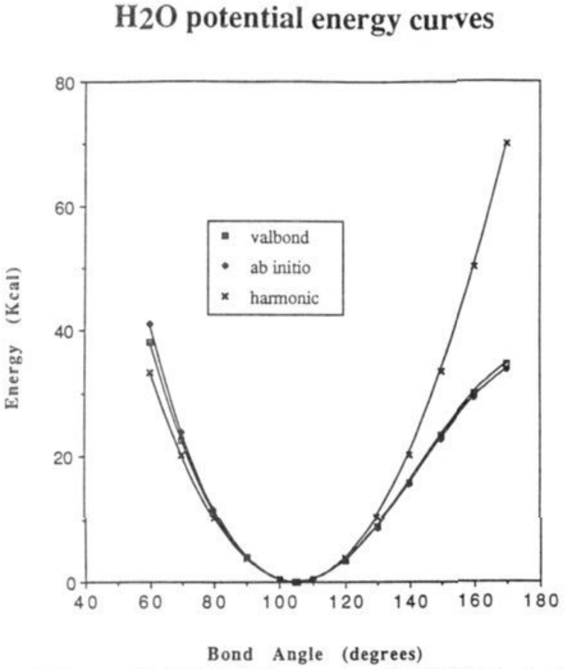

**Figure 2.** Hartree–Fock 6-311G**, harmonic, and VALBOND potential energy curves for $H_2O$.

that orbital and the *positions*, and not the hybridizations, of the other ligands. The different hybridization of, for example, the C–Cl bond is taken into account when the defect of the C–Cl hybrid orbital is computed. Thus, it is the different preferred hybridizations for different ligands that leads to inequal Cl–C–Cl and H–C–Cl bond angles. A general expression for the hybrid strength-based angular potential energy is given in eq 17. Throughout this paper we will refer to a force field using this angular term as the VALBOND force field.

$$E_{\text{tot}} = \sum_{i}^{\text{all ligands}} \sum_{j \neq i} k_i (S_i^{\max} - S_i(\alpha_{ij})) \tag{17}$$

## IV. Assignment of Hybridizations

The VALBOND force field requires hybridization and a scaling parameter ($k$, hereafter referred to as the VALBOND parameter) to be assigned to each ligand. The assignment of gross hybridizations to a central atom, for example, $sp^3$ for chloroform and $sp^2$ for formaldehyde, is intuitive. The assignment of hybridizations to individual bonds is not. Previously, procedures for determining hybridizations for molecules containing inequivalent ligands have been proposed.[19] These procedures typically use experimental geometries along with orthogonality and normalization constraints to generate a set of solvable linear equations. Such procedures are not suitable for implementation in VALBOND because (1) these hybridizations are not necessarily those that will give the correct geometries when minimized using the VALBOND potential energy term and (2) these procedures require that one know the equilibrium geometry and, thus, are not useful for *predicting* molecular shapes.

Our approach uses simple Lewis dot structures and a quantitative expression of Bent's rule to determine individual bond hybridizations. Consider the set of structures shown below. For each of these, we draw the simplest, nonhypervalent Lewis dot representation. For structures **1–4**, the valence electrons occupy all three valence p-orbitals and the valence s-orbital. The gross hybridizations of the central atoms for these examples approximate $sp^3$. For $BH_3$ and ethylene, generation of the localized single bond framework requires just two of the valence p-orbitals; the gross hybridizations are $sp^2$. The gross hybridization assignments use the implicit rules: (1) use as few p-orbitals as possible and (2) each $\pi$-bond occupies a p-orbital of the constituent atoms. But how should the three p-orbitals used in single bonds by structures **1–4** and the two p-orbitals used in single bonds by structures **5** and **6** be distributed among the different ligands, lone pairs, and singly occupied orbitals?


1

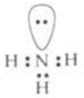
2

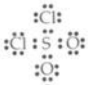
3

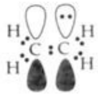
4


5


6

Our hybridization algorithm assumes that each ligand, lone pair, or singly occupied orbital has an intrinsic preference for p-character. Hybridization preferences for different ligands are incorporated as weighting factors. Final distribution of p-character in each of the hybrid orbitals is computed from the weighting factors (wt) and the number of p-orbitals available ($n_p$) (as determined from the gross-hybridization). Application of eq 19 converts from %p character to hybridization ($sp^x$).

$$\%\text{p}_i = \frac{n_p \text{wt}_i}{\sum_{j}^{\substack{\text{ligands,}\\ \text{lone pairs,}\\ \text{radicals}}} \text{wt}_j} \tag{18}$$

$$\%\text{p}_i = \%\text{p character of } i\text{th ligand}$$

$$n_p = \text{no. of p-orbitals used in gross hybridization}$$

$$\text{hybridization of ligand } i = \text{sp}^{\%\text{p}_i/(1-\%\text{p}_i)} \tag{19}$$

Consider the example of propene. The carbon weighting factors for hydrogen and carbon are 1.05 and 1.00, respectively (vide infra for the parametrization methods). Gross hybridizations are $sp^3$ (three p-orbitals are available for $\sigma$ bonding) for the methyl carbon and $sp^2$ (two p-orbitals are available for $\sigma$ bonding) for the vinylic carbons. According to eqs 18 and 19 the individual bond hybridizations are $sp^{3.15}$ and $sp^{2.61}$ for the methyl C–H and C–C bonds, respectively, and $sp^{2.21}$ and $sp^{1.90}$ for the vinyl C–H and C–C bonds, respectively. Although the final energy minimized geometries depend on the values of the VALBOND parameters ($k$) as well as the hybridizations, it is readily seen that the methyl H–C–H bond angles will decrease from 109.47° because the C–H bonds have more p-character than tetrahedral, $sp^3$ hybrid orbitals. Similarly, the vinyl H–C–H bond angle will be less than the trigonal planar value (120°) because the C–H bonds have more p-character than $sp^2$ hybrid orbitals. These qualitative results agree with experiment. Detailed comparisons of computed structures and vibrational frequencies are presented in section VI.

Up to this point we have demonstrated that the nonorthogonality of hybrid orbitals, the pair defect approximation, and a simple algorithm for assigning hybridizations form the basis of a molecular mechanics potential energy term for the description of molecular shapes. In the next section we present the procedures used in parametrizing this potential energy term.

## V. Parametrization and Computational Methods

Of the two parameter types, the VALBOND parameter ($k$, kcal/mol) and the dimensionless hybridization weighting factor (wt), used in generating the VALBOND angular potential energy

---

(19) (a) Grim, S. O.; Plastas, H. J.; Huheey, C. L.; Huheey, J. E. *Phosphorus* **1971**, *1*, 61. (b) Mingos, D. M. P.; Zhenyang, L. *Structure and Bonding* **1990**, *72*, 73.

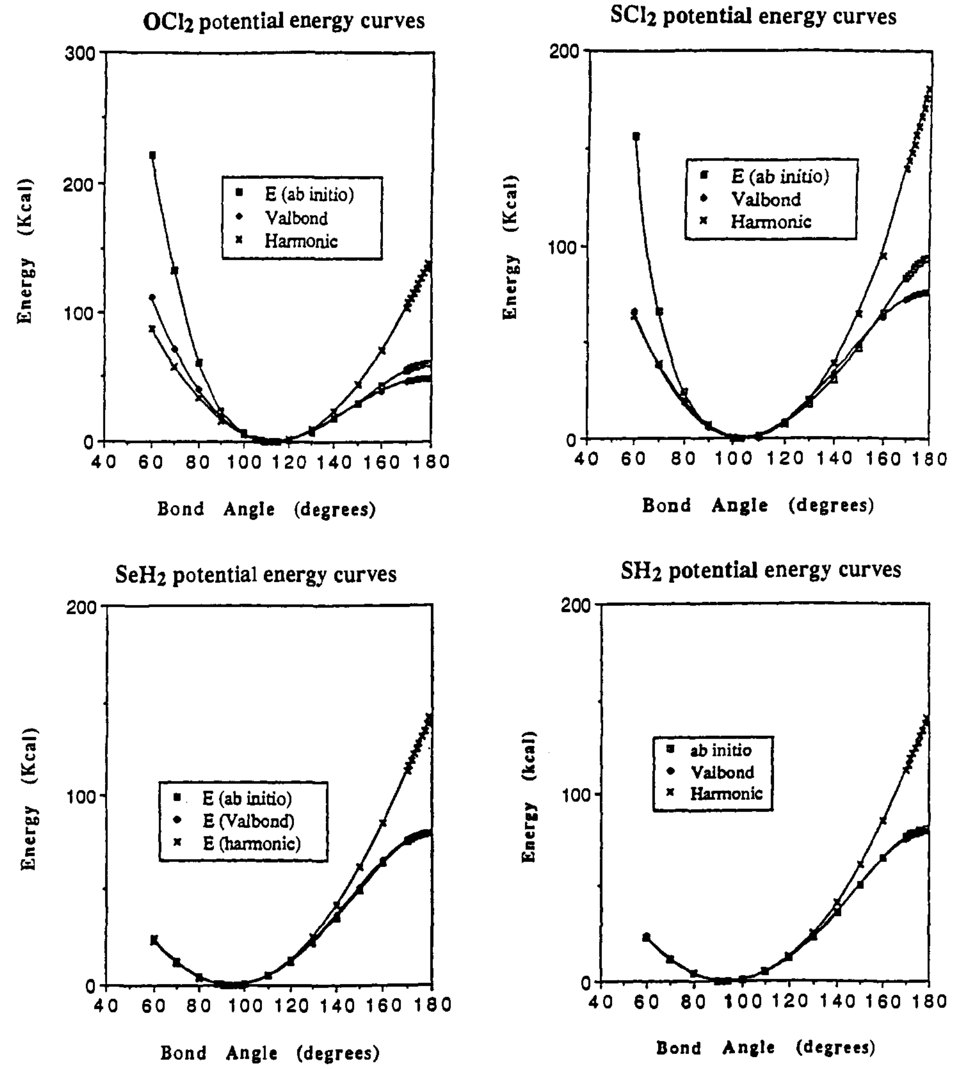

**Figure 3.** Hartree–Fock 6-311G**, harmonic, and VALBOND potential energy curves for $OCl_2$, $SCl_2$, $SeH_2$, and $SH_2$.

term the hybridization weighting factors, exert the greatest influence in determining the final geometry. To a good approximation, the assigned hybridizations determine the shapes (the position of the minima and the curvatures) of the bending potential energy curves in the region of the minima. The VALBOND parameter ($k$) is a linear scaling factor that primarily influences vibrational frequencies and to a lesser extent influences the final equilibrium geometry.

Weighting factors were approximated according to the following rules. (1) A single weighting factor is defined for each combination of elements according to central atom–ligand atom pairs. For example, the carbon–hydrogen weighting factor of 1.05 is used for all C–H bonds regardless of whether the molecule is ethane, benzene, or formaldehyde. (2) In addition, weighting factors are determined for lone pairs and singly occupied orbitals. (3) The weighting factor for a bond between two atoms of the same element is 1.0. (4) For molecules having a known structure and containing a mixture of bonds, lone pairs, or singly occupied orbitals, acceptable weighting factors will generate a minimum for the observed geometry. The criterion for a minimum is that diagonalization of the second derivative matrix generates six eigenvalues of 0.0 and the remaining eigenvalues are positive. For example, $O_3$ has an experimental bond geometry of 116.8° and a simple Lewis structure containing one lone pair on the central oxygen and a resonance mixture of equal parts single and double bond to the terminal oxygens. According to rules 3 and 4, the weighting factor for the lone pair is 0.902. Once a lone pair weighting factor is defined, weighting factors for the O–H bonds of $H_2O$ are readily solved according to rules 1, 2, and 4 yielding a value of 1.016. Similarly, empirical weighting factors may be determined for a wide range of central atom–ligand atom combinations. The weighting factors listed in Table I represent an average over many test structures.

In order to accurately model the energy associated with bond angle distortions, the VALBOND potential energy curves must be scaled. The VALBOND parameters effect this scaling. As with the hybridization weighting factors, we use a single VALBOND parameter for each combination of elements according to central atom–ligand atom pairs. Therefore, the same C–H parameter is used for methane, ethylene, and formaldehyde. Appropriate VALBOND parameter values are determined by matching computed to experimental vibrational frequencies. When computing vibrational frequencies the full force field consisted of the CHARMM potential energy function (eq 1) with the VALBOND angular term (eq 17) substituted for the harmonic CHARMM term. For convenience we will refer to this potential energy expression as the VALBOND force field. Parameter optimization was performed using a simplex procedure that simultaneously adjusted the VALBOND parameters and the bond-stretching force constant to give the best fit between computed and experimental vibrational frequencies. Other required force field parameters (for improper and proper dihedral terms and nonbonded parameters) were taken from the CHARMM/QUANTA[20] parameter file. In some instances minor adjustment of the CHARMM/QUANTA parameters were required.

Ultimately the computed molecular geometries and vibrational frequencies depend on both the hybridization weighting factors

---

(20) QUANTA is a registered trademark of Molecular Simulations, Inc. Version 3.2 was used for this work.

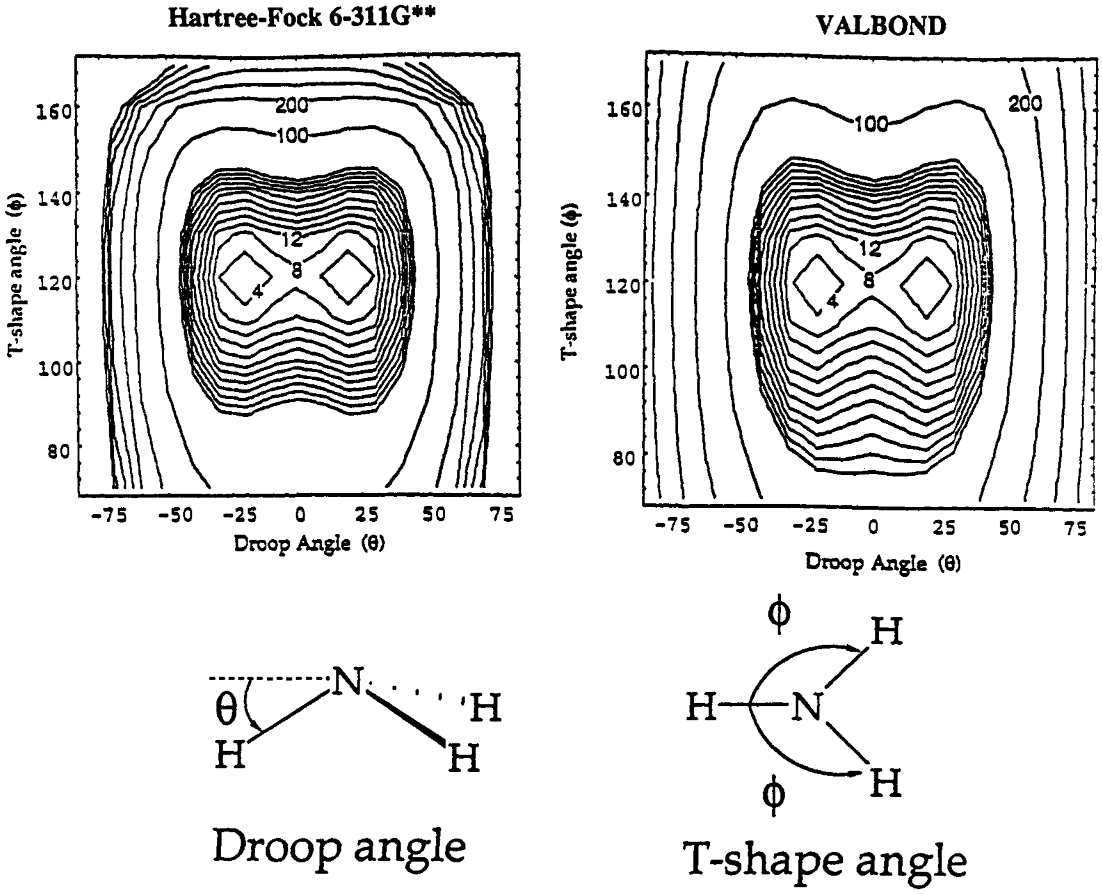

Figure 4. Hartree–Fock 6-311G** and VALBOND potential energy plots for ammonia. The contours are spaced initially by 4 kcal up to 48 kcal. The next contour is at 100 kcal, and the contours are then stepped by 100 kcal.

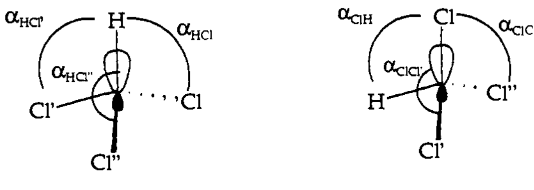

$$E = 1k_H \begin{bmatrix} (s^{max} - s(\alpha_{HCl'})) \\ + \\ (s^{max} - s(\alpha_{HCl''})) \\ + \\ (s^{max} - s(\alpha_{HCl})) \end{bmatrix} + 3k_{Cl} \begin{bmatrix} (s^{max} - s(\alpha_{ClCl'})) \\ + \\ (s^{max} - s(\alpha_{ClCl''})) \\ + \\ (s^{max} - s(\alpha_{ClH})) \end{bmatrix}$$

Figure 5. Application of the pair defect approximation to chloroform. Terms are defined in the text.

and the VALBOND parameters. Therefore a final stage of refinement was used to simultaneously optimize both parameter types. A partial listing of these parameters are given in Table I (further parameters are available as supplementary material). It is interesting to note that the VALBOND parameters do not vary much. In the absence of detailed vibrational analysis default values of ca. 163 kcal/mol for bonds involving H and ca. 220 kcal/mol for all other bonds may be used with good results. In the next section we compare details of computed and experimental molecular geometries and vibrational frequencies.

## VI. Results

Our original intentions in developing the VALBOND force field terms were (1) to model accurately the changes in potential energy associated with angular deformations, (2) to establish a general scheme for predicting approximate equilibrium geometries by using hybridization preferences, and (3) to reduce the number of parameters required to describe a broad range of compound types. In sections II and III we demonstrated the credibility of the VALBOND potential energy function over a wide range of bond angles. We now focus our attention on the latter two points.

Illustrated in Figure 6 are the calculated and observed geometries as well as the computed bond hybridizations for a series of organic molecules with very different bonding schemes and different ligands. A more complete tabulation of computed and observed bond angles is given in Table II for organic molecules and Table III for main group inorganic molecules. All computations used the hybridization weighting factors and VALBOND parameters given in Table I. These results demonstrate the ability of the force field to reproduce subtle variations in molecular geometries. For example, the slightly different H–C–H bond angles of the methyl (108.3°) and methylene (107.2°) groups of propane arise both from the different hybridizations of the C–H bonds ($sp^{3.150}$ for methyl vs $sp^{3.316}$ for methylene) and from different C–C bond hybridizations ($sp^{2.609}$ for methyl vs $sp^{2.727}$ for methylene).

The VALBOND scheme and parameters are versatile; the computed H–C–H bond angles in ethylene, formaldehyde, and singlet and triplet carbene closely match those observed experimentally even though all structures use the same C–H parameters. For these structures the VALBOND hybridization scheme makes subtle changes in the hybridizations of the $\sigma$ bond framework that effect, for example, larger H–C–H bond angles for formaldehyde than for ethylene (see Figure 6). The organic structural parameters given in Table II demonstrate that a wide variety of organic bond angles are reproduced well by the VALBOND force field. Ring structures, aldehydes, esters, amides, ethers, acids, methyl radical, and carbenes are fit well using the same basic set of parameters. Most impressive is the ability of the VALBOND scheme and one set of parameters to generate accurate bond angles about central atoms containing multiple bonds and single bonds. The scheme does break down in some instances, however. For example, the O—C=O angles of esters (ca. 125°) and the N—C=O angles of amides (ca. 122°) are reproduced well but

**Table I.** Weighting Factors (wt) and Valbond Constants (k, kcal·mol$^{-1}$) for Central Atom and Ligand Combinations

| | | ligands | | | | | | | |
|---|---|---|---|---|---|---|---|---|---|
| central atom | | H | B | C | N | O | F | Cl | Br |
| C | wt | 1.05 | 0.958 | 1.0 | 1.0 | 0.875 | 0.99[a] | 0.98 | 0.95 |
| | k | 163 | 220 | 212 | 220 | 220 | 220 | 220 | 220 |
| N | wt | 1.04 | 0.878 | 0.851 | 1.0 | 1.10 | 1.114 | 1.058 | 1.0[b] |
| | k | 145 | 220 | 220 | 190 | 300 | 175 | 220 | 220 |
| O | wt | 1.016 | 0.829 | 0.922 | 1.151 | 1.0 | 1.181 | 0.871 | 1.0[b] |
| | k | 163 | 220 | 220 | 220 | 220 | 195 | 220 | 220 |
| Si | wt | 1.152 | 0.97[a] | 1.114 | 1.005 | 1.01 | 1.251 | 1.18[a] | 0.95 |
| | k | 163 | 220 | 220 | 220 | 220 | 220 | 220 | 220 |
| P | wt | 1.152 | 0.898[a] | 0.97 | 0.397 | 0.342 | 0.442 | 0.437 | 0.402 |
| | k | 122 | 220 | 220 | 220 | 220 | 200 | 220 | 220 |
| S | wt | 1.177 | 0.993 | 0.929 | 1.155[a] | 0.7 | 0.65[a] | 0.871 | 1.0[b] |
| | k | 146 | 220 | 220 | 220 | 220 | 220 | 220 | 220 |

[a] Weighting factor determined by extrapolation. [b] Default weighting factors.

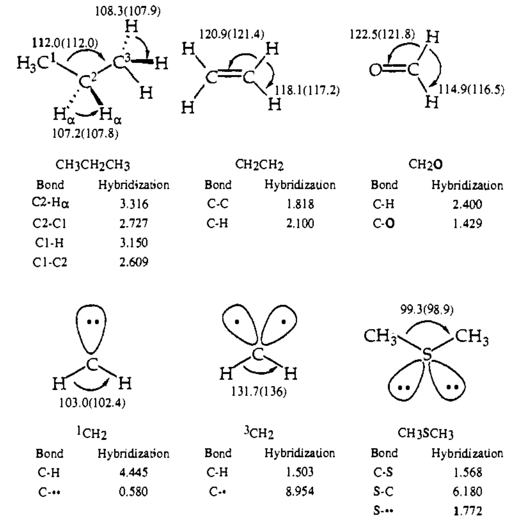

$CH_3CH_2CH_3$

| Bond | Hybridization |
|---|---|
| C2-Hα | 3.316 |
| C2-C1 | 2.727 |
| C1-H | 3.150 |
| C1-C2 | 2.609 |

$CH_2CH_2$

| Bond | Hybridization |
|---|---|
| C-C | 1.818 |
| C-H | 2.100 |

$CH_2O$

| Bond | Hybridization |
|---|---|
| C-H | 2.400 |
| C-O | 1.429 |

$^1CH_2$

| Bond | Hybridization |
|---|---|
| C-H | 4.445 |
| C-•• | 0.580 |

$^3CH_2$

| Bond | Hybridization |
|---|---|
| C-H | 1.503 |
| C-• | 8.954 |

$CH_3SCH_3$

| Bond | Hybridization |
|---|---|
| C-S | 1.568 |
| S-C | 6.180 |
| S-•• | 1.772 |

**Figure 6.** Computed and observed (observed in parentheses) bond angles (deg) and computed bond hybridizations (eq 18) of $CH_3CH_2CH_3$, $CH_2CH_2$, $CH_2O$, $^1CH_2$, $^3CH_2$, and $CH_3SCH_3$. The symbols C-•• and C-• represent doubly and singly occupied orbitals, respectively. These are used for determining hybridizations and do not contribute to the computed energy of a molecule. References to experimental bond angles are given in Tables IV and V.

only at the expense of obtaining O–C–H and O–C–C bond angles that are systematically too large by about 4°. Weighting factors for C–O bonds that yield good descriptions of carbonyl carbon centers cannot simultaneously yield good bond angles about alcoholic carbon centers.

The VALBOND scheme permits a simple treatment of lone pairs and radicals. Singly occupied orbitals and lone pairs are assigned unique weighting factors. The presence of a radical or lone pair influences the geometry solely via the distribution of p-orbital character to the bonded atoms; lone pairs and radicals are *not* included in the computation of the potential energy. Thus, pseudoatoms are not required for computations involving these nonbonding electrons. Singlet and triplet carbenes are modeled simply as electron deficient Lewis structures having one doubly occupied lone pair hybrid on a carbon with sp$^2$ gross hybridization and two singly occupied hybrids on a carbon with sp$^3$ gross hybridization, respectively. Structures for a series of carbenes and methyl radical are included in Table II. The computed bond angles for singlet methylene and triplet methylene trace the observed trend: the triplet has a bond angle that is 30° larger than that of singlet. This is due to the greater preference of a singly occupied hybrid orbital for p-character as compared with a lone pair hybrid orbital. For methyl radical this preference results in a trigonal planar geometry without resorting to improper dihedral constraints. The VALBOND force field predicts a very low-energy (51 cm$^{-1}$) distortion mode for pyramidalization of the methyl radical.

The observed and computed vibrational data for simple organic molecules agree well (see Table IV), even though the same set of weighting factors and VALBOND parameters are used for each molecule. Note also that the VALBOND force field does not contain any off-diagonal terms. For ethane and ethylene the rms deviation of computed and observed vibrational frequencies of ethylene and ethane are 85 and 82 cm$^{-1}$, respectively. Comparison values for the MM3 force field are 68 and 126 cm$^{-1}$, respectively. The rms deviations of computed and observed vibrational frequencies for formaldehyde are large (171 cm$^{-1}$); this probably reflects an unoptimized balance of the C–O VALBOND parameter and hybridization weighting factor. A closer examination of ethane (with sp$^3$ gross hybridization) and ethylene (with sp$^2$ gross hybridization) demonstrates an important property of the VALBOND term: ***the different in-plane bending frequencies of sp$^3$ and sp$^2$ hybridized central atoms can be accounted for by the different curvatures of the hybrid orbital strength functions.*** For example, the curvature of the sp$^2$ strength function is lower than that of the sp$^3$ function leading to lower energy H–C–H bending modes for ethylene relative to methane. This property allows the same VALBOND (or scaling) parameter to be used for a C–H regardless of the hybridization of the carbon.

The VALBOND treatment of angular terms results in a significant reduction of parameters as compared with other molecular mechanics force fields. Consider the number of parameters required to generate the angular potential energy terms of the VALBOND force field and a pure diagonal force field, such as CHARMM, for the set of molecules comprising propyne, propene, propane, formaldehyde, dimethyl ether, and methyl acetate. The CHARMM force field requires 20 equilibrium bond angles and 20 force constants to generate the angular potential energy terms, whereas the VALBOND force field requires just four weighting factors and four VALBOND parameters (C–C, C–O, C–H, O–C). The UFF force field developed by Rappé, Casewit, and co-workers[3] achieves a more drastic reduction of angular parameters by using a variant of Badger's rules for computing force constants and limiting equilibrium bond angles to those of a few idealized geometries. Excellent results are obtained with UFF although some of the more subtle variations in bond angles are not reproduced. Vibrational data have not been reported for the UFF force field.

The VALBOND scheme is readily extended to simple main group inorganic molecules (see Table III). As with organic compounds, radicals (e.g., $NO_2$) as well as closed shell molecules are described well by a single set of weighting factors and VALBOND parameters. In general, bond angles are reproduced to within two degrees. In some instances the VALBOND scheme breaks down. For example, the H–N–Cl bond angles of $NHCl_2$ and $NH_2Cl$ are overestimated by about four degrees. A single N–H weighting factor and a single N–Cl weighting factor cannot fit the 107° bond angles of $NCl_3$ and $NH_3$ and also yield 102° bond angles for H–N–Cl. For B, C, N, and O it may be necessary to add 1,3-interaction terms that better simulate the ligand–

**Table II.** Computed and Observed Bond Angles (deg) for Organic Molecules

| molecule | angle | VALBOND | experimental |
|---|---|---|---|
| $^1CH_2$ | H-C-H | 103.0 | 102.4[a] |
| $^3CH_2$ | H-C-H | 131.7 | 136[a] |
| $CH_3$ | H-C-H | 120 | 120[a] |
| $^1CF_2$ | F-C-F | 103.8 | 104.8[a] |
| $^1CHF$ | H-C-F | 103.6 | 101.8[a] |
| $^1CCl_2$ | Cl-C-Cl | 103.9 | 100(9)[a] |
| ethane | H-C-H | 108.3 | 107.5(1.0)[b] |
| | C-C-H | 110.6 | 111.2(0.3) |
| propane | C-C-C | 112.0 | 112.0(0.2)[b] |
| | $H\text{-}C_{(2°)}\text{-}H$ | 107.2 | 107.8(0.2) |
| butane | C-C-C | 112.0 | 113.3(0.4)[c] |
| isobutane | C-C-C | 110.7 | 110.8(0.2)[c] |
| cyclopentane ($C_s$) | C2-C1-C5 | 103.7 | 103.0[d] |
| | C1-C2-C3 | 104.9 | 104.2 |
|  | C2-C3-C4 | 106.4 | 105.9 |
| cyclohexane | C-C-C | 110.7 | 111.4(0.2)[c] |
| | H-C-H | 107.7 | 107.5(0.2) |
| methylcyclohexane | C-C-C(exo) | 110.9 | 112.1(1.6)[c] |
| nobornane | C1-C2-C3 | 102.4 | 102.7[e] |
| | C2-C1-C6 | 109.0 | 109.0 |
| 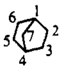 | C1-C7-C4 | 91.8 | 93.4 |
| ethylene | C=C-H | 120.9 | 121.4(0.6)[f] |
| propene | C=C-C | 122.8 | 124.3(0.8)[f] |
| | C=C-H | 118.7 | 121.3(0.1) |
| | =C-C-H | 110.4 | 116.7(0.3)[b] |
| *cis*-2-butene | C-C=C | 124.9 | 125.4(0.4)[f] |
| cyclopentene | C3-C2=C1 | 111.9 | 111.0[f] |
| | C2-C3-C4 | 104.9 | 103.0 |
| 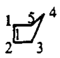 | C3-C4-C5 | 106.3 | 104.0 |
| cyclohexene | C-C=C | 123.0 | 124.0(0.2)[f] |
| cyclohexadiene | C-C=C | 123.2 | 122.7[f] |
| | C-C-C | 113.6 | 113.3 |
| norbornene | C1-C7-C4 | 93.4 | 95.3[f] |
| 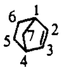 | C1-C2=C3 | 106.7 | 107.7(MM3)[f] |
| methanol | O-C-H(trans) | 112.8 | 107.2[a] |
| | H-C-H | 105.4 | 108.5 |
| 1,4-dioxane | C-C-O | 112.5 | 109.2(0.5)[g] |
| | C-O-C | 111.7 | 112.6(0.5) |
| formaldehyde | O-C-H | 122.5 | 121.8[h] |
| | H-C-H | 114.9 | 116.5 |
| acetaldehyde | C-C-O | 123.9 | 124.7(0.2)[b] |
| | C-C-H | 115.4 | 113.9(0.2) |
| acetone | C-C-C | 116.0 | 116.0(0.2)[b] |
| | C-C=O | 122.0 | 122.0(0.2) |
| methyl formate | O-C=O | 125.9 | 125.9[h] |
| | C-O-C | 111.9 | 114.8 |
| acetic acid | C-C=O | 117.6 | 126.6[h] |
| | C-C-O | 117.5 | 110.6 |
| | O=C-O | 124.6 | 123.0 |
| methylactate | C-O-C | 115.1 | 114.8[h] |
| piperazine | C-C-N | 110.8 | 109.8(0.5)[g] |
| | C-N-C | 113.8 | 112.6(0.5) |
| nitromethane | ⟨N-C-H⟩ | 109.8 | 107.2[h] |
| succinamide | N-C-O | 121.4 | 122[h] |
| | C-C-N | 114.0 | 116 |
| | C-C=O | 124.5 | 122 |
| acetamide | N-C-C | 117.5 | 115.1(1.6)[h] |

[a] Hehre, W. J.; Pople, J. A.; Radom, L.; Schleyer, P. R. *Ab Initio Molecular Orbital Theory*; Wiley: New York, 1986. [b] Smith, J. C.; Karplus, M. *J. Am. Chem. Soc.* **1992**, *114*, 801. [c] Allinger, N. L.; Yuh, Y. H.; Lii, J. *J. Am. Chem. Soc.* **1989**, *111*, 8551. [d] Saebo, S.; Cordell, F. R.; Boggs, J. E. *J. Mol. Struct.* (*Theochem*) **1983**, *104*, 221. [e] Allinger, N. L.; Geise, H. J.; Pyckhout, W.; Paquette, L. A.; Gallucci, J. C. *J. Am. Chem. Soc.* **1989**, *111*, 1106. [f] Allinger, N. L.; Li, F.; Yan, L. *J. Comput. Chem.* **1990**, *11*, 848. [g] Davis, M.; Hassel, O. *Acta Chem. Scand.* **1963**, *17*, 118. [h] Hellwege, K.-H. *Landolt-Boernstein Numerical Data and Functional Relationships in Science and Technology*; Springer Verlag: Berlin, 1976; Vol. 17. Broken brackets indicate quantities averaged over all such terms.

ligand Pauli repulsions that occur when ligand atoms are large and ligand-to-central atom bonds are short. The equilibrium

**Table III.** Computed and Observed Bond Angles (deg) for Main Group Inorganic Molecules

| molecule | angle | VALBOND | experimental |
|---|---|---|---|
| $BHF_2$ | F-B-F | 118.1 | 118.3[a] |
| $BHCl_2$ | Cl-B-Cl | 119.6 | 119.7[a] |
| $BF_2NH_2$ | F-B-F | 119.9 | 117.9[a] |
| | H-N-H | 115.0 | 116.9 |
| $NH_3$ | H-N-H | 106.8 | 106.7[a] |
| $NCl_3$ | Cl-N-Cl | 106.5 | 107.1[a] |
| $NHCl_2$ | H-N-Cl | 106.7 | 102[b] |
| | Cl-N-Cl | 106.1 | 106 |
| $NH_2Cl$ | H-N-H | 107.1 | 106.8[b] |
| | H-N-Cl | 106.3 | 102 |
| $[N_3]^-$ | N-N-N | 180 | 180[b] |
| $NO_2$ | O-N-O | 129.5 | 134.1[a] |
| NClO | Cl-N-O | 114.2 | 113.3[a] |
| $PH_3$ | H-P-H | 93.8 | 93.3[a] |
| $PCl_3$ | Cl-P-Cl | 100.1 | 100.1[a] |
| $CH_3PH_2$ | C-P-H | 97.1 | 96.5[a] |
| | H-P-H | 91.3 | 93.4 |
| $(CH_3)_3PH$ | C-P-C | 98.5 | 99.7[a] |
| | C-P-H | 95.6 | 97.0 |
| $(CH_3)_3P$ | C-P-H | 95.6 | 98.6[c] |
| $AsH_3$ | H-As-H | 91.7 | 92.1[a] |
| $AsF_3$ | F-As-F | 96.0 | 96.0[a] |
| $AsCl_3$ | Cl-As-Cl | 98.7 | 98.6[a] |
| $AsBr_3$ | Br-As-Br | 99.6 | 99.7[a] |
| $AsI_3$ | I-As-I | 100.2 | 100.2[a] |
| $O_3$ | O-O-O | 116.8 | 116.8[a] |
| $(CH_3)_2O$ | C-O-O | 111.6 | 111.7[a] |
| $(CH_3)_2S$ | C-S-C | 99.3 | 98.9[a] |
| $(CH_3)_2Se$ | C-Se-C | 96.2 | 96[a] |
| $(SiH_3)_2O$ | Si-O-Si | 142.7 | 144.1[a] |
| $(SiH_3)_2S$ | Si-S-Si | 99.6 | 97.4[a] |
| $(SiH_3)_2Se$ | Si-Se-Si | 98.0 | 96.6[a] |
| $(GeH_3)_2O$ | Ge-O-Ge | 126.2 | 126.5[a] |
| $(GeH_3)_2Se3$ | Ge-Se-Ge | 94.1 | 94.6[a] |
| $Si_4O_4C_8H_{24}$ | Si-O-Si | 143.4 | 142.5[a] |
| 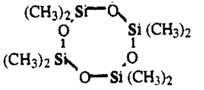 | O-Si-O | 112.4 | 109 |
| | C-Si-C | 107.3 | 106 |
| $Ge_4S_6(CF_3)_4$ | ⟨S-Ge-S⟩ | 113.8 | 113.8[a] |
| 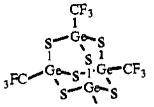 | ⟨Ge-S-Ge⟩ | 99.9 | 99.9 |
| $Sn_6(Ph_2)_6$ | ⟨Sn-Sn-Sn⟩ | 112.4 | 112.5[a] |
| 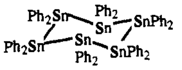 | C-Sn-C | 105.5 | 106.7 |
| $B_3Ph_3O_3$ | ⟨B-O-B⟩ | 121.8 | 121.7[a] |
| 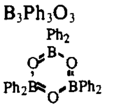 | ⟨O-B-O⟩ | 118.2 | 118.0 |
| $PO_4P_3O_3$ | $O_1\text{-}P_1\text{-}O_2$ | 114.1 | 115[a] |
| 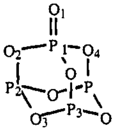 | $O_2\text{-}P_1\text{-}O_4$ | 104.5 | 103 |
| | $O_2\text{-}P_2\text{-}O_3$ | 99.3 | 99 |
| | $P_1\text{-}O_2\text{-}P_2$ | 122.9 | 124 |
| | $P_2\text{-}O_3\text{-}P_2$ | 127.3 | 128 |
| $Ga_2Pyr_2Br_4$ | Br-Ga-Br | 107.0 | 105.8[a] |
| 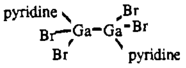 | Ga-Ga-Br | 115.1 | 116.3 |
| $As_3(CH_3)_6In_3(CH_3)_6$ | C-In-C | 101.9 | 99[a] |
| 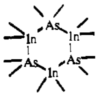 | C-As-C | 124.7 | 126 |

[a] Hellwege, K.-H. *Landolt-Boernstein Numerical Data and Functional Relationships in Science and Technology*; Springer Verlag: Berlin, 1976; Vol. 7. [b] *Tables of Interatomic Distances and Configuration in Molecules and Ions*; Sutton, L. E., Ed.; Special Publication No. 11; The Chemical Society: London, 1958. [c] Allinger, N. L.; Von Voithenberg, H. *Tetrahedron* **1978**, *34*, 627. Broken brackets indicate quantities averaged over all structures.

**Table IV.** Computed and Observed Vibrational Frequencies ($cm^{-1}$) of Methane, Ethane, Ethylene, and Formaldehyde

| no. | symm | calcd | obsd | no. | symm | calcd | obsd |
|---|---|---|---|---|---|---|---|
| Methane ($T_d$)[a] | | | | | | | |
| 1 | $T_2$ | 2982 | 3020 | 6 | E | 1553 | 1499 |
| 2 | $T_2$ | 2982 | 3020 | 7 | $T_2$ | 1386 | 1337 |
| 3 | $T_2$ | 2982 | 3020 | 8 | $T_2$ | 1386 | 1337 |
| 4 | $A_1$ | 2820 | 2914 | 9 | $T_2$ | 1386 | 1337 |
| 5 | E | 1553 | 1499 | | | | |
| | | | | | | RMSD | 53.7 |
| Ethane ($D_{3d}$)[b] | | | | | | | |
| 1 | $E_u$ | 2983 | 2947 | 10 | $E_g$ | 1536 | 1469 |
| 2 | $E_u$ | 2983 | 2947 | 11 | $A_{1g}$ | 1568 | 1388 |
| 3 | $E_g$ | 2978 | 2950 | 12 | $A_{2u}$ | 1475 | 1370 |
| 4 | $E_g$ | 2978 | 2950 | 13 | $E_g$ | 1081 | 1190 |
| 5 | $A_{1g}$ | 2877 | 2915 | 14 | $E_g$ | 1081 | 1190 |
| 6 | $A_{2u}$ | 2867 | 2915 | 15 | $A_{1g}$ | 874 | 995 |
| 7 | $E_u$ | 1520 | 1460 | 16 | $E_u$ | 909 | 822 |
| 8 | $E_u$ | 1520 | 1460 | 17 | $E_u$ | 909 | 822 |
| 9 | $E_g$ | 1536 | 1469 | 18 | $A_{2u}$ | 312 | 279 |
| | | | | | | RMSD | 82.4 |
| Ethylene ($D_{2h}$)[c] | | | | | | | |
| 1 | $B_{2u}$ | 3106 | 3106 | 7 | $A_g$ | 1197 | 1342 |
| 2 | $B_{1g}$ | 3100 | 3103 | 8 | $B_{1g}$ | 1000 | 1222 |
| 3 | $A_g$ | 3013 | 3026 | 9 | $A_u$ | 1094 | 1023 |
| 4 | $B_{3u}$ | 2988 | 2989 | 10 | $B_{2g}$ | 1033 | 943 |
| 5 | $A_g$ | 1660 | 1623 | 11 | $B_{1u}$ | 948 | 949 |
| 6 | $B_{3u}$ | 1405 | 1444 | 12 | $B_{2u}$ | 812 | 826 |
| | | | | | | RMSD | 85.1 |
| Formaldehyde ($C_{2v}$)[d] | | | | | | | |
| 1 | $B_1$ | 2870 | 2874 | 4 | $A_1$ | 1343 | 1503 |
| 2 | $A_1$ | 2804 | 2780 | 5 | $B_1$ | 893 | 1280 |
| 3 | $A_1$ | 1762 | 1744 | 6 | $B_2$ | 1169 | 1167 |
| | | | | | | RMSD | 171 |

[a] Decius, J. C. *J. Chem. Phys.* **1948**, *16*, 222. [b] Schachtschneider, J. H.; Snyder, R. G. *Spectrochim. Acta* **1963**, *19*, 117. [c] Ermer, O.; Lifson, S. *J. Am. Chem. Soc.* **1973**, *95*, 4121. Barnes, A. J.; Howells, J. D. R. *J. Chem. Soc., Faraday Trans. 2* **1973**, *69*, 532. [d] Herzberg, G. *Infrared and Raman Spectra of Polyatomic Molecules*; D. Von Norstrand Company, Inc.: New York, 1945.

**Table V.** Calculated[a] and Observed[b] Vibrational Frequencies ($cm^{-1}$) for $C_{3v}$ $AsX_3$ (X = H, F, Cl, Br, I)

| no. | symm | calcd | obsd | no. | symm | calcd | obsd |
|---|---|---|---|---|---|---|---|
| $AsH_3$[c] | | | | | | | |
| 1 | E | 2123 | 2123 | 4 | E | 1009 | 1003 |
| 2 | E | 2123 | 2123 | 5 | E | 1009 | 1003 |
| 3 | $A_1$ | 2122 | 2116 | 6 | $A_1$ | 996 | 907 |
| | | | | | | RMSD | 36.6 |
| $AsF_3$[d] | | | | | | | |
| 1 | E | 726 | 644 | 4 | $A_1$ | 290 | 343 |
| 2 | E | 726 | 644 | 5 | E | 279 | 274 |
| 3 | $A_1$ | 706 | 715 | 6 | E | 279 | 274 |
| | | | | | | RMSD | 52.4 |
| $AsCl_3$[e] | | | | | | | |
| 1 | E | 439 | 307 | 4 | $A_1$ | 167 | 194 |
| 2 | E | 439 | 307 | 5 | E | 158 | 155 |
| 3 | $A_1$ | 411 | 412 | 6 | E | 158 | 155 |
| | | | | | | RMSD | 77.2 |
| $AsBr_3$[f] | | | | | | | |
| 1 | E | 303 | 275 | 4 | $A_1$ | 129 | 128 |
| 2 | E | 303 | 275 | 5 | E | 117 | 98 |
| 3 | $A_1$ | 277 | 284 | 6 | E | 117 | 98 |
| | | | | | | RMSD | 19.8 |
| $AsI_3$[g] | | | | | | | |
| 1 | E | 237 | 221 | 4 | $A_1$ | 80 | 94 |
| 2 | E | 237 | 221 | 5 | E | 70 | 70 |
| 3 | $A_1$ | 208 | 216 | 6 | E | 70 | 70 |
| | | | | | | RMSD | 11.5 |

[a] All frequencies were computed with a force field consisting of bond stretch and VALBOND angle terms. [b] Ross, S. D. *Inorganic Infrared and Raman Spectra*; McGraw Hill: London, 1972; pp 173–174. [c] The stretching force constant and VALBOND parameter for $AsH_3$ are 190 and 110 kcal/mol, respectively. [d] The stretching force constant and VALBOND parameter for $AsF_3$ are 330 and 180 kcal/mol, respectively. [e] The stretching force constant and VALBOND parameter for $AsCl_3$ are 185 and 180 kcal/mol, respectively. [f] The stretching force constant and VALBOND parameter for $AsBr_3$ are 130 and 250 kcal/mol, respectively. [g] The stretching force constant and VALBOND parameter for $AsI_3$ are 95 and 160 kcal/mol, respectively.

geometry of siloxane is fit well, and the VALBOND potential energy curve exhibits a low "inversion" barrier (that is the barrier to achieving a linear geometry) of 1.3 kcal/mol (0.3 kcal/mol experimental).[21] These results suggest that VALBOND should accurately describe the geometries and dynamics of zeolites.

Computed and experimental vibrational frequencies for a series of $C_{3v}$ *As*(III) molecules are listed in Table V. Excellent agreement is found despite the pure-diagonal nature of the VALBOND force field. We have computed the following inversion barriers for the $NH_3$, $PH_3$, $AsH_3$, and $SbH_3$: 6.6 kcal/mol (5.8 kcal/mol experimental), 30.8 kcal/mol (32.2 kcal/mol experimental), 33.6 kcal/mol (44 kcal/mol experimental), and 31.1 kcal/mol (38 kcal/mol experimental), respectively. Without the inclusion of an improper dihedral term the VALBOND force field underestimates the stibine and arsine inversion barriers by about 20%.

## VII. Conclusions

Chemists are accustomed to discussing qualitative aspects of molecular geometries in terms of hybridization. In this paper we have shown that a detailed theory of directed covalent bond orbitals forms the basis of a quantitative description of molecular shapes that is suitable for implementation in a molecular mechanics force field. The cornerstone of the VALBOND scheme is the generalized strength function for two equivalent orbitals having any arbitrary hybridization. Equilibrium molecular geometries are those which minimize the defects of the hybrid orbitals that bond the central atom to its ligands. For molecules that have inequivalent ligands, defects are approximated by pairwise summations. Another building block of the VALBOND scheme is the algorithm for assigning hybridizations. Implicit to our algorithm is the assumption that different ligand atoms, lone pairs, and radical electrons have intrinsic relative preferences for p-character. This assumption combined with Lewis structure-based allocations of electron pairs leads to a parametrized method for assigning hybridizations to each ligand bond, lone pair, and radical electron associated with a central atom. Structures and vibrational frequencies computed using the VALBOND force field and the hybridization algorithm agree well with experimental values. As compared with other molecular mechanics force fields, VALBOND achieves comparable accuracies in the computations of bond angles and vibrational frequencies but with far fewer parameters.

Our future work will involve the extension of these hybridization schemes for the description of the molecular shapes of hypervalent main group molecules and transition metal complexes.

**Acknowledgment.** This work was supported by the National Science Foundation (CHE9112988) and a gift from the 3M Corporation. We appreciate receiving from Prof. Tony Rappé manuscripts describing the UFF force field prior to their publication. Mr. Dan Filo's assistance with programming is gratefully acknowledged.

**Supplementary Material Available:** Table of the VALBOND parameters and hybridization weighting factors for the p-block of the periodic table (2 pages). Ordering information is given on any current masthead page.

---

(21) Durig, J. R.; Flanagan, M. J.; Kalasinsky, V. F. *J. Chem. Phys.* **1977**, *66*, 2775.